Construction and Building Materials 262 (2020) 120475

Contents lists available at ScienceDirect

Construction and Building Materials

journal homepage: www.elsevier.com/locate/conbuildmat

Up-scaling and performance assessment of façade panels produced from construction and demolition waste using alkali activation technology

Ana Frankovič [a], Vilma Ducman [a,*], Sabina Dolenec [a], Matteo Panizza [b], Sergio Tamburini [b], Marco Natali [b], Maria Pappa [c], Constantinos Tsoutis [c], Adriana Bernardi [d]

[a] Slovenian National Building and Civil Engineering Institute, Dimičeva ulica 12, 1000 Ljubljana, Slovenia
[b] National Research Council of Italy (CNR), Institute of Condensed Matter Chemistry and Technologies for Energy (ICMATE), Corso Stati Uniti 4, 35127 Padua, Italy
[c] Proigmenes Erevnitikes & Diahiristikes Efarmoges (AMSolutions), Dim. Glinou 7, Irakleio 14122, Greece
[d] National Research Council (CNR), Institute of Atmospheric Sciences and Climate (CNR-ISAC), Corso Stati Uniti 4, 35127 Padua, Italy

HIGHLIGHTS

- Optimization and analysis of the alkali activated mixtures were performed.
- Laboratory and scale-up (pilot) productions of façade panels were conducted.
- The durability behaviour of façade panels from both types of production was investigated.

ARTICLE INFO

Article history:
Received 11 July 2019
Received in revised form 12 July 2020
Accepted 1 August 2020
Available online 29 August 2020

Keywords:
CDW
Alkali activated material
Geopolymer
Façade panels
Pilot production
Durability
Circular economy

ABSTRACT

Novel prefabricated insulating façade panels were developed from construction and demolition waste (CDW) aggregates under the framework of the European H2020 project InnoWEE. These non-structural components, aimed at improving the thermal efficiency of existing buildings, consist of an insulating plate covered by a facing layer made of CDW aggregates bound with metakaolin, furnace slag and class F fly ash activated by a potassium silicate solution. The paper presents the design and assessment of the binder and panels for exterior use, taking into account mechanical performance, behaviour in the presence of water and durability issues. Testing was carried out on both laboratory prototypes and panels from the pilot industrial production.

1. Introduction

Construction and demolition waste (CDW) represents about one third of all generated waste in the European Union [1], and in some countries this is still sent to landfills. The composition of this type of waste, however, offers the potential for it to be reused in the construction industry. It was therefore determined under Directive 2008/98/EC that from 2020 a minimum of 70% of nonhazardous CDW must be recycled [2]. These materials primarily consist of brick, concrete, tile and other ceramics, while approximately one third are made up of other construction materials, such an asphalt, stone, wood. Such CDW can be recycled into aggregate which has a positive environmental impact by reducing the consumption of natural aggregates and minimizing exploitation of non-renewable raw materials [3].

One of the most promising and innovative ways to reuse the largest amount of industrial waste and CDW is alkali activation technology, which uses various secondary raw materials (e.g. fly ash, blast furnace slag, metakaolin and red clay brick) as aluminosilicate precursors, which are then chemically activated by different alkali sources [4–6]. Some authors, for instance, have successfully developed alkali activated mortars or concretes where a high content of CDW was used as either an aggregate [7–9] or as a binder component [10–13]. The compressive strength of synthesis mixtures reached 40 MPa in both cases, and was influenced by various

* Corresponding author.
E-mail addresses: ana.frankovic@zag.si (A. Frankovič), vilma.ducman@zag.si (V. Ducman), sabina.dolenec@zag.si (S. Dolenec), matteo.panizza@icmate.cnr.it (M. Panizza), sergio.tamburini@icmate.cnr.it (S. Tamburini), marco.natali@icmate.cnr.it (M. Natali), maria.pappa@amsolutions.gr (M. Pappa), constantinos.tsoutis@amsolutions.gr (C. Tsoutis), a.bernardi@isac.cnr.it (A. Bernardi).

https://doi.org/10.1016/j.conbuildmat.2020.120475
0950-0618/

parameters including the precursor ratio, the type and molarity of the activator, and curing temperature. Furthermore, a mixture of waste glass powder, NaOH, and water (an alternative to commercial sodium silicate), can be used as the alkali source in order to further reduce the CO_2 footprint and cost of alkali activated material (AAM) [14–16].

An important property of materials for outdoor use is their resistance to environmental factors, such as acid rain, moisture, freezing, and overheating. It has been reported that AAM exhibit superior resistance to sulphate (Na_2SO_4) and acid attack in comparison to ordinary concrete, which decomposes when exposed to these conditions due to a change in the phenomenon of calcium silicate hydrate (CSH) decalcification [17,18]. Conversely, exposure of AAM to $MgSO_4$ solution could cause degradation of the AAM binder [19]. Nazari et. al. [20] reported that the compressive strength of AAM even increased after exposure to high temperatures (up to 400 °C), and following thermal shocks it preserved better mechanical properties in comparison to ordinary concrete. Studies have shown that the influence of natural carbonatization on the deterioration of alkali activated pastes depends on the AAM composition and the pore diameter. The investigation showed a decrease in resistance of alkali activated fly-ash - slag mixtures to carbonatization compared to alkali activated slag only [21]; the same phenomenon occurred in mixtures activated with Na_2SiO_3 [22]. When considering materials for outdoor use freeze–thaw resistance is another important durability property. Sun et. al. [23] confirmed the high freeze–thaw resistance of fly-ash based mortars after 300 freeze–thaw cycles. Based on the results available from the experimental work, it can be concluded that the freeze–thaw resistance of AAM mostly depends on air content, air void distribution, water-to-binder ratio, activator type, temperature, and the duration of the freeze–thaw cycles [24].

Due to the significant effort of the European Union to increase energy savings in old buildings [25] new façade retrofitting solutions are constantly being developed. Franzoni et. al., for example, developed prefabricated external thermal insulation composite panels with a porcelain stoneware rendering layer [26]. Panels were shown to have a high resistance to fire, the rendering layer exhibited high durability, and assembly time was shortened due to the prefabricated nature of their design.

The objective of this study was to develop a suitable alkali activated formulation including CDW which could be used in the building sector for production of façade panels as part of the InnoWEE project (Innovative prefabricated components including different waste construction materials which reduce building energy and minimise environmental impact). Both laboratory scale and pilot production of such panels took place in order to confirm the feasibility of such production, define the parameters for upscaling, and provide enough panels to be investigated both in a laboratory setting as well as when installed on demo sites in the field.

2. Materials and methods

2.1. Raw materials

The solid precursors used in the binder were commercial metakaolin (MK: M1000 from Imerys, France) with a volume median diameter D_{50} = 15.6 μm, commercial granulated blast furnace slag (SL: LV425 supplied by Minerali Industriali, Italy), with D_{50} = 9 μm, and fly ash (FA: type EFA Füller HP supplied by BauMineral GmbH, Germany) with D_{50} = 18 μm, as reported in their respective data sheets. Table 1 indicates the quantitative chemical analysis of each material by energy dispersive X-ray spectrometry (EDS), as carried out by a FEI Quanta 200F FEG-ESEM equipped with an EDAX Genesis EDS system.

In the first phase of the research, an in-house prepared potassium silicate activator with molar modulus $SiO_2/K_2O \approx 2.3$ and dry matter concentration of 42% was used. The candidate mixtures were then manufactured using an activator derived from a commercial product (Crosfield, Italy), which had a molar modulus SiO_2/K_2O of 1.9 and concentration of 45% (d_{20} = 1.513 g/cm^3). The presence of Na_2O, commonly found in commercial K-silicates owing to the frequent use of the same reactors to produce Na-silicates, was lower than 1%.

Aggregates used for AAM production came from inorganic non-hazardous CDW obtained by the selective demolition of buildings carried out by an Italian company which operates in the field of recycled aggregates and is part of the InnoWEE consortium. The same company were also responsible for the waste processing. Input CDWs were classified as either 17.01.01 (concrete), 17.01.07 (mixtures of concrete, brick, tile and other ceramics), or 17.09.04 (mixed construction and demolition waste), according to the European List of Wastes [27]. Mixed scraps, primarily destined for road backfilling, were ground to obtain recycled sands with a maximum nominal size of 2 mm. Indicative ranges of the main constituents are reported in Table 2, based on bulk chemical analysis carried out on separated concrete and fired clay materials [7]. It is worth highlighting that the use of a blend of concrete and fired clay waste allowed the issues related to the release of Cr by recycled concrete aggregates to be overcome. According to the leaching test provided by the standard EN 12457–2 [28], recycled concrete aggregates tested alone did not meet the limit set by Italian regulations to permit its transformation into a secondary raw material (SRM), as pointed out by tests carried out in the framework of the InnoWEE project. Further discussion of this aspect can be found in [7].

2.2. Laboratory preparation of binders and panel prototypes

Binders were prepared by stirring solid precursors and the alkali activator together in a planetary mixer for about 5 min, before adding the waste aggregates and plastic short fibres (polypropylene 6 mm long). It should be noted that the moisture content of ingredients (MK, SL, FA and waste aggregates) cannot be feasibly assessed at the moment of mixing. Nonetheless, raw materials were stored under rather constant conditions, assuring moisture fluctuations lower than 0.2%. When required, the casting of specimens for mechanical and physical characterization was promoted by external pneumatic ball vibrators.

Panel prototypes of size 500 × 500 mm^2 were manufactured by pouring an alkali activated layer into the bottom of a mould fastened to a stiff plate, sometimes covered in advance with a plastic or rubber insert to impress the facing texture. After vibration to expel possible air bubbles, a mesh (i.e. a glass-fibre mesh for mortar renders) was placed on the mould and immersed into the AAM. An insulation layer (an expanded polystyrene – EPS – plate) was then pressed against the mixture with the aid of vibration to force contact. Finally, a stiff plate was placed on top as a lid and clamped to the mould. After further vibration, the system was placed in a sealed plastic bag and cured at 50 °C for 12 h.

2.3. Upscaling production of external thermal insulation composite system (ETICS) like panels – Pilot production

After extensive testing of laboratory made panels, the panels were further optimised within the pilot production (Fig. 1).

A step-by-step upscaling methodology was developed, based on industrial techniques and tools, through use of the Define, Measure, Analyse, Improve and Control (DMAIC) method, part of the 6σ methodology. The 6σ methodology can be defined as a set of quality management methods and statistical methods, fostering a

Table 1
Elemental analysis of oxides (% weight) for metakaolin (MK), granulated blast furnace slag (SL), and fly ash (FA).

Material	Al_2O_3	SiO_2	CaO	Fe_2O_3	K_2O	MgO	SO_3	TiO_2
MK	41.47	53.26	–	1.97	1.18	–	–	1.95
SL	9.31	36.48	44.36	0.57	0.71	6.20	1.55	0.83
FA	24.81	50.51	6.52	7.16	2.51	2.32	1.72	1.43

Table 2
Indicative range of the main constituents of CDW aggregates, based on the analysis of separated materials [7]

SiO_2	CaO	Al_2O_3	MgO	Fe_2O_3
40–60%	8–40%	5–15%	3–12%	2–5%

dedicated infrastructure of people within the organization who are experts in their individual fields [29]. Once the laboratory tests were completed and the prototypes developed, the results were analysed, optimized and finally converted into a generic document, the "Basic Flow Sheet", which aims to be a guideline for any future upscaling. The key task was to convert the outcome of the "Basic Flow Sheet" to a "Detailed Design", with modelling simulations for all the production-critical tasks and their engineering implementation to a flexible "modular" production line in the Technology Upscaling Pilot Plant (TUPP) in Greece.

The pilot production included the following steps: filling liquid silicate in the mixer, feeding solid raw materials to a premixing buffer, premixing with polypropylene fibres, transferring solid raw materials to the main mixer, mixing, casting, panel assembly, curing, demoulding, post-curing, eventual painting and cleaning (Fig. 2).

200 ETICS-like panels were produced in the pilot plant (TUPP). Table 3 shows the total amount of raw materials used to synthesize the AAM mixture for the production of the final panels, as well as the quantity of EPS and glass mesh.

The whole process is divided into 5 phases. Phase 1 is the preparation of raw materials which is mainly the modification of the commercial K-silicate solution from 2.0/45.2% to 1.9/45% by addition of the appropriate amount of KOH solutions. Phase 2 is the main HDA production process, which includes premixing the solid raw materials (metakaolin, slag and fly ash) and then mixing those materials with the K-sil activator 1.9/45% in a mechanical mixer. The next step is the addition of the fine and coarse CDW to the mixture and then the gradual addition of the polypropylene fibres. After mixing until completely homogeneous, the mixture is transferred to the casting area (phase 3). There, the appropriate amount of AAM mixture is added to the moulds and the system is vibrated until the mixture in the mould is completely levelled. Next, the fiberglass net is applied to the mixture and the EPS panel is then placed on the mould and the system is vibrated. The system is secured then inserted into a sealed bag, a humidity agent is added and finally the bag is firmly sealed. Phase 4 involves inserting the sealed moulds into the oven for curing at 50 °C, demoulding, and then curing at r.t. The last phase (phase 5), consists of painting the panels, packaging and storage or distribution.

2.4. Test methods

As there are no standard test methods available for prefabricated alkali activated composite façade panels, the developed panels were assessed by provisions from the European Technical Assessment Guide (ETAG 004) [32] and other European standards, with some modifications where necessary. All exposures and measurements were carried out on samples after curing for 28 days at 23 °C and 50% RH.

Viscosity in laboratory conditions was measured with a rotational viscometer (Brookfield DV2T with spindle n°5 at 1 rpm) equipped with a temperature probe.

AAM samples, embedded in epoxy resin by vacuum impregnation, cut transversally, and polished, were subjected to complete microstructural and microchemical characterization by scanning electron microscopy and energy-dispersive microanalysis (SEMEDS). A CamScan MX2500 scanning electron microscope was used, equipped with a LaB6 cathode and an EDAXEDS energy dispersive Xray fluorescence spectrometer, with data acquired at an accelerating voltage of 20 kV.

The density, porosity and pore size distribution of the rendering layer were determined by means of Mercury intrusion porosimetry (MIP). A sample of approximately 5 × 5 × 5 mm in size was cut from the rendering layer, dried in an oven for 24 h at 70 °C, and analysed with Autopore IV 9500 (Micromeritics) equipment. The

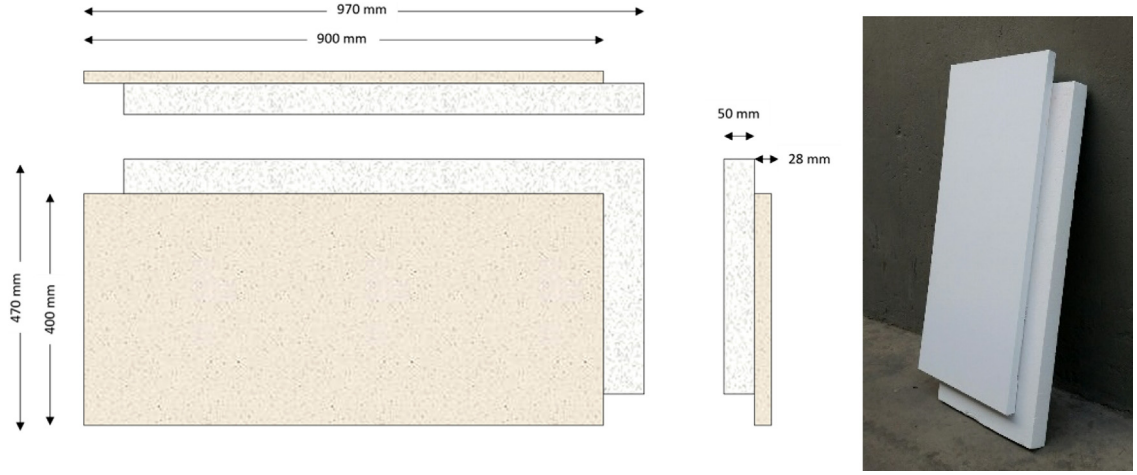

Fig. 1. Sketch of the ETICS-like panel (left), and a sample produced in the Technology Upscaling Pilot Plant (TUPP).

Fig. 2. The "modular" production line.

Table 3
Total quantities of raw materials used for the up-scale production of 200 ETICS-like panels.

Total amount of materials used for the production of alkali-activated material for 200 ETICS-like panels	
Materials	Mass (kg)
Metakaolin	228.71
Slag	152.18
Fly ash	76.09
K-silicate	450.12
CDW fine	246.96
CDW coarse	370.99
KOH 90%	6.23
Water	6.55
Polypropylene Fibres	2.16
Total amount of additional materials used for the production of 200 ETICS-like panels	
Materials	Mass (kg)
EPS	138.6
Glass mesh	11.14

contact angle was 130°, Hg surface tension was 0.485 N/cm and Hg density was 13.53 g/ml.

The drying shrinkage of binders was measured on cylinders 160 mm long with a nominal diameter of 22 mm, placed vertically inside specially designed frames which supported a digital dial gauge (resolution 1 μm, accuracy 3 μm) mounted in contact with the top end of the specimen. The bottom end was supported by a spherical restraint corresponding to the central axis of the cylinder. Specimens were monitored continuously for at least the first 2–7 days, then removed and occasionally replaced for at least 1–2 days. A reference mark was taken to ensure the position of the samples did not change.

The compressive strength of binders was measured on cylindrical specimens with a nominal diameter of 22 mm and 2:1 aspect ratio, tested by means of a universal multipurpose frame (Matest Unitronic S205) equipped with a 50 kN load cell. Tests were carried out in displacement control, with a movable beam rate of 0.5 mm/min.

Capillary water absorption was determined according to ETAG 004 on three 200 × 200 mm samples cut from panels from the laboratory and pilot production [30]. The edges of samples were sealed with silicon to prevent water penetrating between the rendering AAM layer and the insulation layer. Water uptake was measured at intervals of 3 min (zero reading), 1 h and 24 h.

In order to determine the permeability of the façade panels' rendering layer to water vapour, the "dry cup" method according to EN ISO 7783 [31] was used. The cup contained a solution of lithium chloride (LiCl). The measurements were performed on two samples with a 340 cm^2 surface area, after 28 days of curing under laboratory conditions.

The bond strength between the rendering layer and insulation was determined according to ETAG 004 [30] on panels of dimensions 400 × 200 mm. Five circles of 50 mm diameter were cut approximately 1 cm deep through the rendering layer into the insulation layer. Sikadur 31CF RAPID adhesive was used to bond the steel dolly onto the samples. Bond strength was determined by a portable dynamometer Freundl F15D EASY M, which operates within a pulling capacity of up to 15 kN.

Freeze-thaw resistance was assessed according to ETAG 004 [30] on two panels of dimensions 500 × 500 mm (the whole panel) and 400 × 200 mm (panel cut into half) from the laboratory and pilot production, respectively. The samples were exposed to 30 cycles as follows: (i) immersed in water for 8 h at an initial temperature of 23 ± 2 °C; and (ii) freezing at – 20 ± 2 °C for 14 h. Visual inspection was made after the cycles and bond strength was determined.

The impact resistance of developed panels was determined according to standard ISO 7892 [33] on two test samples – one sample was a whole panel, and the second was half the façade panel. Two different steel balls were used in the tests, a lighter one causing a 3 Joule impact when dropped from a height of 0.63 m and a heavier one giving a 10 Joule impact when dropped from a height of 1.02 m. Following visual inspection of the damage incurred, the panels were categorised into impact categories according to ETAG 004 [30].

Resistance to carbonation was determined on two AAM samples with dimensions 30 × 30 × 160 mm according to standard EN 13295:2004 [34]. The depth of carbonation was measured before exposure to 1% CO2 (RH 60 ± 10%) and after 7, 28 and 56 days of exposure. Freshly broken faces of prisms were sprayed with phenolphthalein indicator solution which contained 1 g of phenolphthalein indicator, 70 ml of ethanol and 30 ml of dem-

ineralised water. The depth of CO_2 penetration was determined visually.

Resistance to freezing in the presence of deicing salt was determined according to standard SIST 1026 [32] on three 100 × 100 mm samples from the laboratory and three 100 × 100 mm samples pilot production after 28 days curing in laboratory conditions. A 3% solution of NaCl was used as a defrosting agent. The surface is considered resistant to freezing if delaminated material does not exceed the limit value after 25 cycles. NaCl solution was poured into moulds around the samples to a height of approximately 35 mm, and left for 7 days in laboratory conditions. After 7 days of conditioning, the freeze–thaw cycles commenced: (i) freezing at – 20 ± 2 °C for 16 h, and (ii) thawing in laboratory conditions (21 °C) for 8 h.

Sulphate resistance was determined on two samples of dimensions 30 × 30 × 160 mm according to ASTM C1012/C1012M-09 [36]. After 28 days curing under laboratory conditions the samples were stored in saturated limewater for 28 days. Afterwards, the samples were exposed to Na_2SO_4 at 23 °C. Standard ASTM C 227–10 [35] was used to investigate potential alkali silica reactivity. Two samples of dimensions 30 × 30 × 160 mm were used for measurements. Before exposure in a chamber at 38 °C, samples had been cured under laboratory conditions for 28 days.

3. Results and discussion

3.1. Laboratory development of alkali activated mixtures and laboratory panels

3.1.1. Adjustment of fluidity and open time of the binders

Alkali activated mixtures incorporating high amounts of CDW and possessing suitable physical/ mechanical characteristics to be used in building elements have been presented in a previous study. Based on those formulations, a further investigation was carried out focusing on fluidity and open time, aimed at achieving features compliant for pilot production in line with the requirements of the pilot plant. The open time is herein defined as the time span from the beginning of the reaction to the loss of pourability, and was qualitatively estimated by visual observation.

As discussed in [7], a higher curing temperature was shown to accelerate strength gain. Furthermore, higher temperatures reduce drying shrinkage, as shown in Fig. 3, which refers to samples manufactured with a preliminary mixture. Nonetheless, since the beneficial effect was less remarkable above 50 °C, this value was selected as the best trade-off to minimize energy cost.Fig. 4.

The investigation to reduce viscosity started with mixtures made from an in-house prepared K-silicate activator with a molar ratio Si_2O/K_2O of 2.3 and a dry matter concentration of 42%. The reference binder had nominal molar ratios Si/Al of 2.4 and K/Al of 0.66, which accounts for the moles of Si and K coming from the K-silicate solution and the moles of Si and Al contained in all the precursors, i.e. MK, SL and possibly FA, not including waste aggregates [37]. Indeed, a possible reactivity of waste was discussed in [7], where aggregates from concrete and fired clay rubble were tested either separately or mixed in various proportions. Those results suggested that the presence of fired clay in the blend offered a beneficial effect compared to the use of concrete only, but the mechanism was effective locally, at the aggregate interface. Owing to the particle size distribution of the processed waste, which cannot be considered finely ground (particles larger than 0.063 mm composed about 96–98% of the recycled aggregates weight), a significant participation of waste aggregates in the alkali activation reaction can be conservatively disregarded. The Si_2O/K_2O modulus of the K-silicate activator and the K/Al ratio of the reference binder were set on the basis of preliminary trials, and through adjustment of these parameters an open time of about 1 h at 20 °C was successfully achieved.

The reference mixtures, with or without fly-ash, were set to have a rather low viscosity (approximately 200 Pa·s at 18 °C), while retaining their thixotropic behaviour. A suitable range for the initial viscosity of mixtures has been previously studied and found to be in the range 1000 – 2000 Pa·s. Values lower than approximately 800 Pa·s allowed the mixture to be poured by gravity. Fluidity was increased to obtain mixtures which could be poured by gravity. The reduction of viscosity was achieved in two ways. Firstly, by increasing the amount of extra water added during mixing, since no effective superplasticizer was found for this kind of binder. The addition of extra water increases porosity and consequently reduces the strength [39]. Moreover, it facilitates the segregation of aggregates, since coarser fractions tend to sink and fines tend to emerge. A second approach was thus considered, which entailed increasing the amount of alkaline activator to approximately equate the quantity of extra water previously added through solvated water contained in the K-silicate solution, thus increasing the K/Al ratio.

The precursor to activator to aggregate proportions by weight were as follows: Series "A": MK:SL:FA:CDW:Ksil ≈ 1.00:1.00:0:2.71:1.75; series "B": MK:SL:FA:CDW:Ksil ≈ 1.00:0.50:0.50:2.71:1.75. In A2b and B2b, the amount of k-silicate was 2.15 instead of 1.75. Water content, Si/Al and K/Al molar ratios of the tested mixtures are listed in Table 4.

Indeed, a second approach to extend the open time took into account the use of fly ash, according to previous literature [38]. The partial replacement (50%) of furnace slag with class F fly-ash had a limited effect on strength (between –9% and + 10%), as shown in Fig. 5, which also compares the measured initial viscosity. Values in the range 80–100 Pa·s implied a strength range of approximately 32–50 MPa. The overall best performance in terms

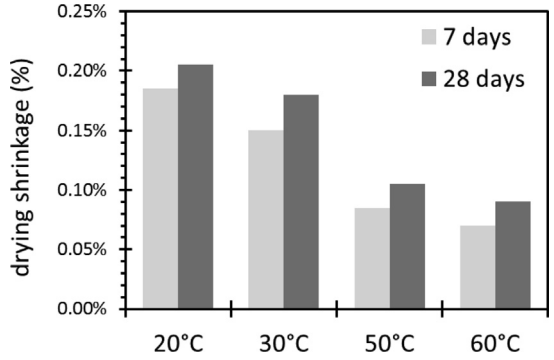

Fig. 3. Drying shrinkage as a function of curing temperature.

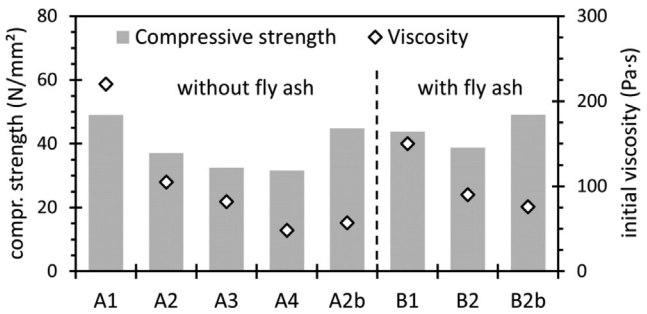

Fig. 4. Fluid mixtures compared in terms of compressive strength and initial viscosity.

Table 4
Water content and K/Al ratio of mixtures for the preliminary study on viscosity and open time.

Mixture	A1	A2	A3	A4	A2b	B1	B2	B2b
H_2O content	20.9%	23.1%	23.8%	25.4%	22.8%	20.9%	23.1%	22.8%
Si/Al molar ratio	2.4	2.4	2.4	2.4	2.6	2.1	2.1	2.2
K/Al molar ratio	0.66	0.66	0.66	0.66	0.81	0.55	0.55	0.68

of fluidity and strength was provided by mixtures with a greater K/Al molar ratio (i.e. A2b and B2b).

During this phase of the research, all test samples were prepared with both the ingredients and the mixer held at a temperature of approximately 20 °C, based on the outcomes of a previous study [7] that involved slightly different viscous binders. By increasing the temperature of the alkali activated paste to 20–30 °C, it was observed that open time decreased substantially, i.e. from more than 30 min to less than 10 min. In the case of the present fluid mixtures it can be noted that the addition of fly-ash had a beneficial effect, leading to mixtures which were workable for hours. Nonetheless, a minimum open time of about 1 h was observed in all cases, as shown in Fig. 6, which also reports values of drying shrinkage measured at 7 and 28 days, ranging between 0.10 and 0.15%.

3.1.2. Development and microstructural characterization of the final binder

Panel prototypes were prepared in parallel with the development of fluid binders. Heuristic observations of the behaviour of prototypes revealed issues largely related to excessive differential deformations and cracking (Fig. 6). In particular, cracking was imputed to drying shrinkage that induced tensile stresses, probably not effectively counteracted by the limited early tensile strength of the mixtures. In addition, differential deformations were observed also in specimens with a rather uniform desiccation, and they were ascribed to a likely excessive segregation of aggregates during the casting phase, which required vibration. Indeed, preliminary trials showed that drying shrinkage in mixtures with predominantly fine aggregates was considerably bigger than in mixtures with mostly coarser aggregates, by as much as 50% higher or more.

For these reasons, the following countermeasures were taken to define the final binder: (i) reduction of water content to slightly reduce the fluidity and to limit the segregation of aggregates; (ii) increase in potassium content to improve the strength; (iii) addition of short plastic fibres (1.5‰ of total dry weight) to minimise improve behaviour against shrinkage-induced cracks [39]; (iv) use of two types of recycled sand blended in 2:1 proportion by weight - a coarser one with aggregate size in the range 1–2 mm and a finer one in the range 0–1 mm.

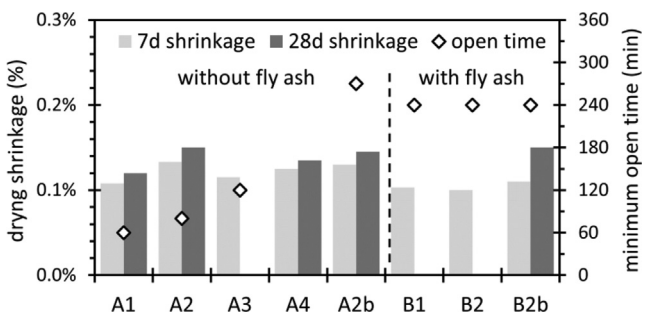

Fig. 5. Fluid mixtures compared in terms of drying shrinkage and qualitative open time.

Quantities of the ingredients were finally set in the following proportions, rounded to 2 significant figures by weight: MK:SL:FA:CDW:Ksil = 3.0:2.0:1.0:8.1:6.1, using a K-silicate with molar ratio $SiO_2/K_2O \approx 1.9$ and a concentration of 45%. The water content, with reference to the overall dry weight, was 19.9%. Based on the chemical composition of the solid precursors and activator, not including CDW aggregates and not making assumptions about the possible partial reactivity of furnace slag and fly ash, the nominal molar ratios were as follows: Si/Al ~ 2.2, K/Al ~ 0.80. At about 23 °C, the fresh mixture exhibited a viscosity of between 120 and 150 Pa·s and an open time greater than 70 min, evaluated through the increase in rate of viscosity. The hardened mixture had an average 28-day compressive strength of approximately 38 N/mm^2 and an apparent density of about 1.89 g/cm^3 in environmental conditions (room temperature).

Samples of the final mixture, which contained a blend of concrete and fired clay aggregates, were characterized by a microstructure consisting of a dense matrix of partially-reacted alkali-activated binder cementing the CDW particles, broken by sporadic shrinkage microcracks. Particles of unreacted fly ash and furnace slag can be observed, indicating the incomplete reaction of these alkali activated components, but only a few unreacted metakaolin particles remained. Partially unreacted slag particles have an important role as the matrix skeleton. The reacted matrices show a compositional homogeneity, with significant amounts of calcium (Fig. 7) higher near the slag particles, indicating higher reaction features in the slag particles.(See Fig. 8.)

Detailed observations of the interfacial transition zones between the binding matrix and the CDW particles showed clear dissolution features of the aggregate in a hyperalkaline environment, modifying the local chemical composition of the matrix in terms of Ca/Si ratio reduction (Fig. 9), which can be imputed to a release of Si from the surface of the fired clay aggregates, producing a significant increase in adhesion between the components Fig. 10.

3.2. Mixture and product samples testing in up-scale production

During pilot production, there is a series of mandatory Audit Tasks that need to be performed in order to ensure not only the repeatability of the formulation but also the quality of the finished product. Various parameters have been tested during the audits and the most important of those are the viscosity of the alkali activated paste, water absorption and hardness.

The viscosity of the alkali activated paste is the most crucial factor influencing the overall production process. Samples were therefore taken from two different production modules: a) from the main mixer, once mixing of the alkali activated paste was complete (prior to its transportation to the filling station) and b) from the filling station, in the middle of the scheduled batch production. According to modelling simulations, the optimum viscosity values are between 600 and 1200 cP. As illustrated in Fig. 11, the viscosity pattern indicates that the viscosity values vary slightly between the mixer and the filling station. This is an expected situation, as the time lapse between the two samples is on average 20–25 min, during which time the solidification of the alkali activated paste is in progress. The dotted lines (green and blue) represent an

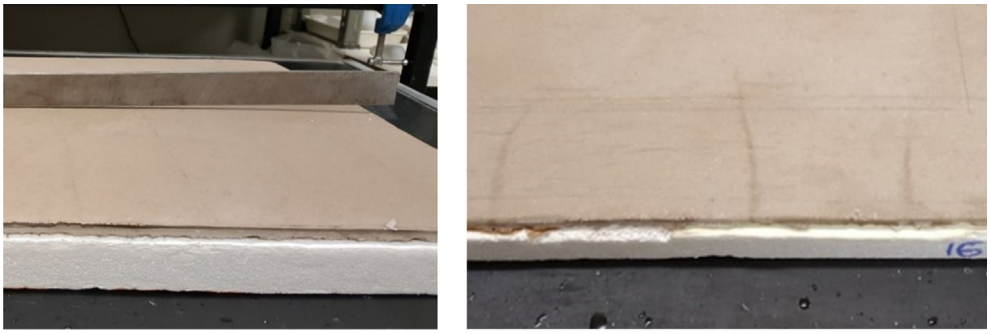

Fig. 6. Example of deviation from planarity (a) and thin cracks highlighted by wetting the surface (b).

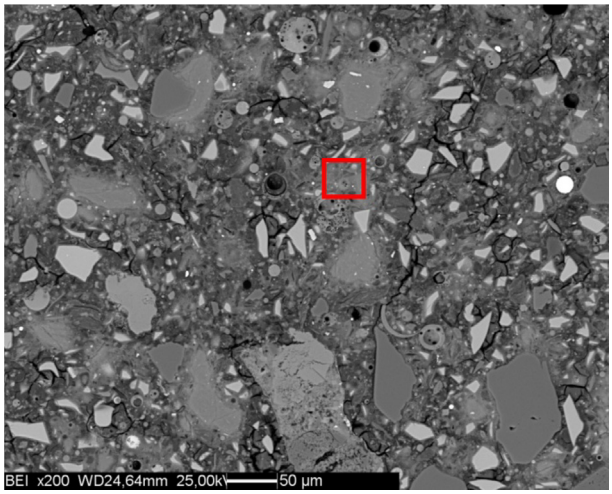

Fig. 7. SEM/BSE micrograph.

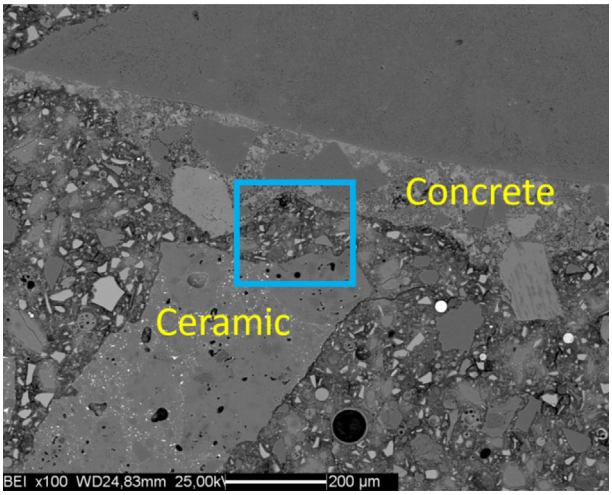

Fig. 9. SEM micrograph (backscattered electrons signal).

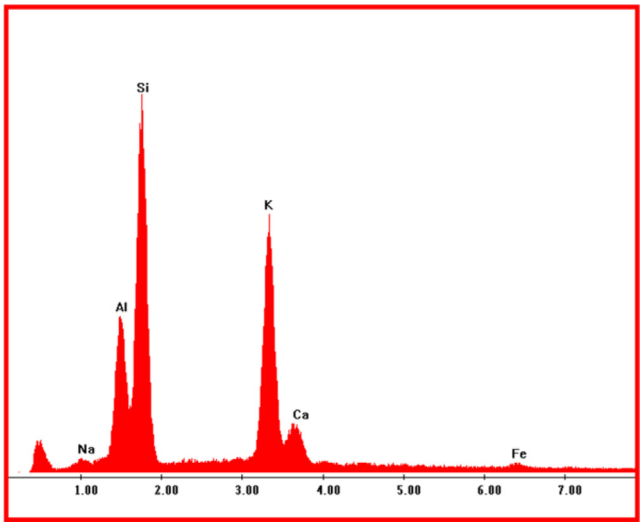

Fig. 8. EDS microanalysis of the area highlighted in Fig. 7.

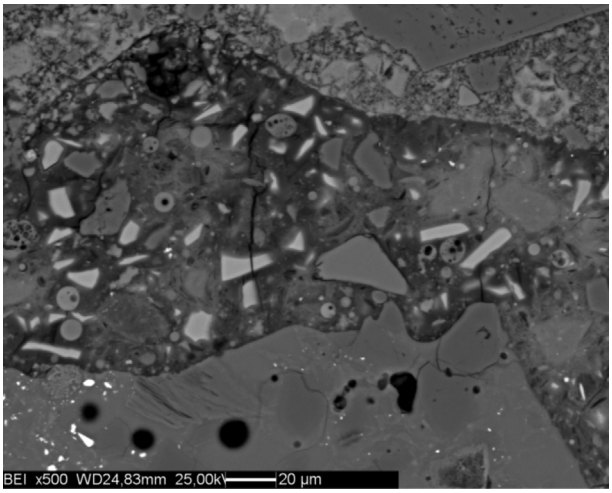

Fig. 10. Magnification of the area highlighted in Fig. 9.

on the spot measurement taken with a portable viscosity meter, which should not be considered accurate values but were rather indicative values to facilitate decision making during production.

The main conclusions of water absorption tests (Fig. 12) are as follows: a) in the 1st and 3rd batch trials the obtained values exceeded the acceptable range of values as determined by the laboratory test results and the modelling simulations; b) after the 3rd trial batch, all values were recorded within the acceptable value range, and c) as production was evolving, the values tended to reach the levels of the laboratory values, indicating a constant improvement of the HDA (High Density AAM) properties. It has to be underlined that the water absorption test is a rather time consuming test for industrial standards (a duration of more than

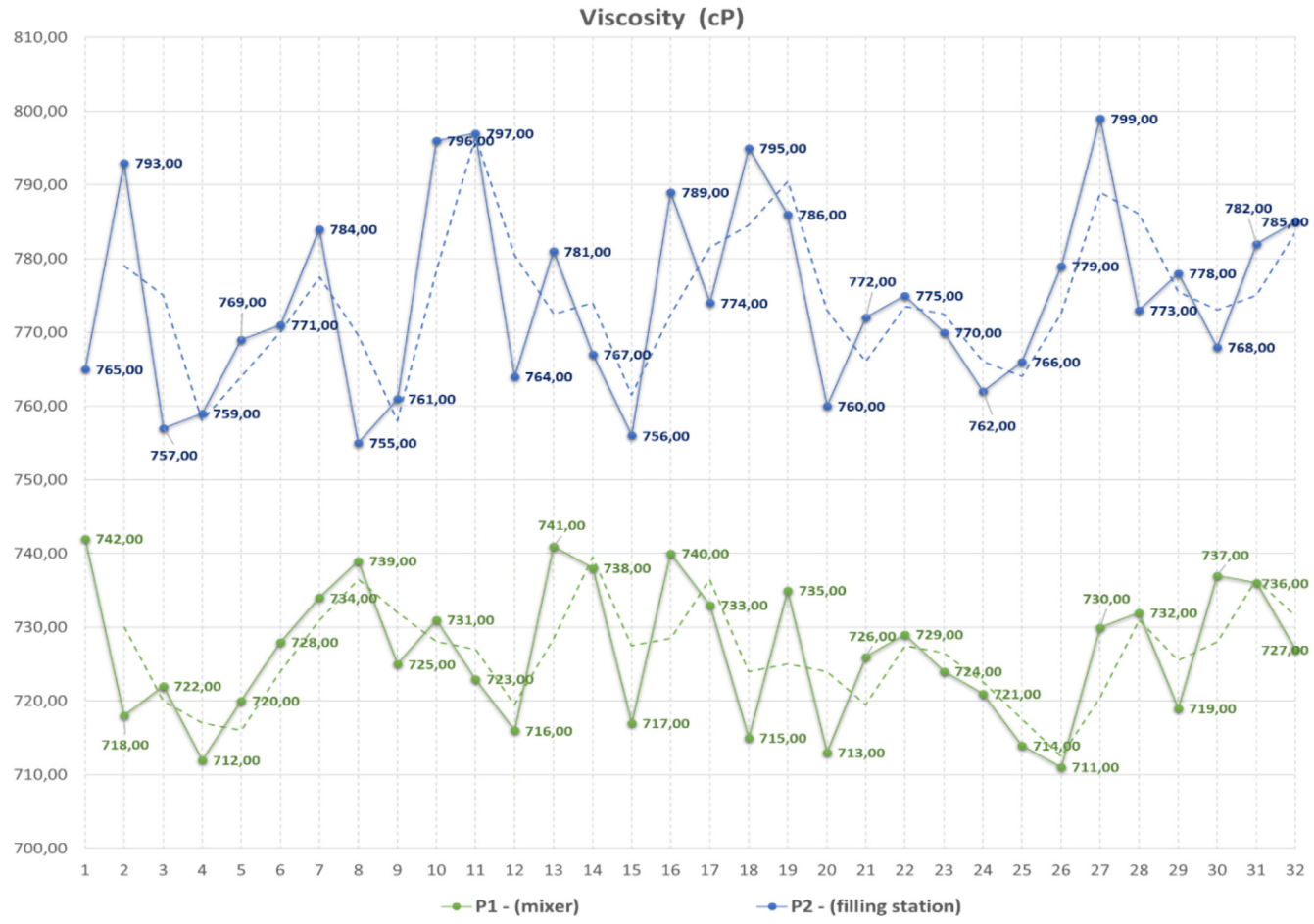

Fig. 11. Viscosity pattern of HDA paste per batch.

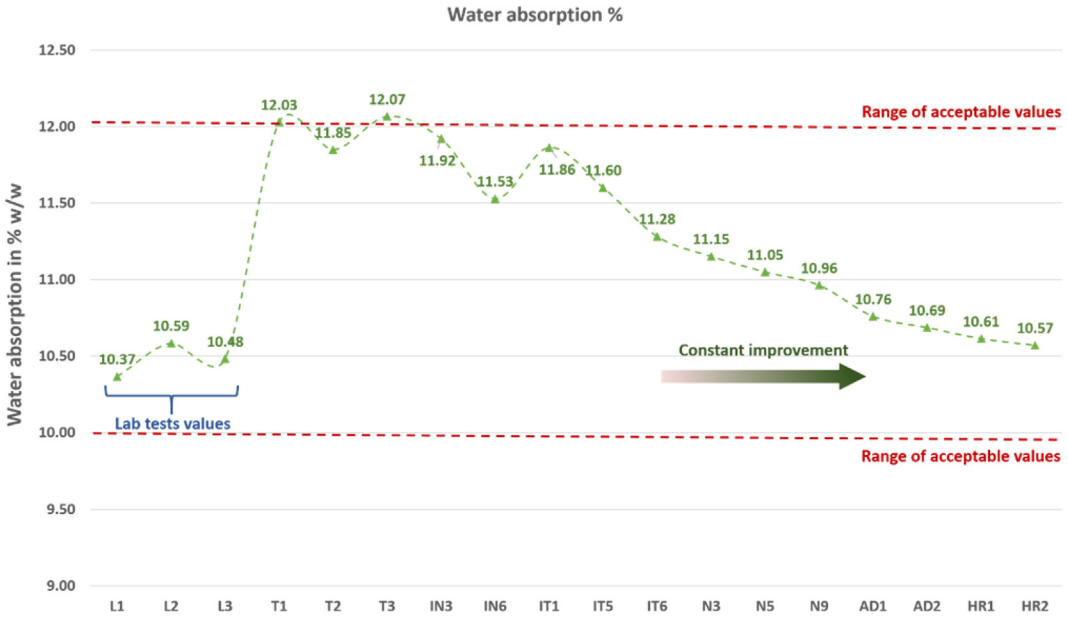

Fig. 12. Water absorption values pattern.

24 h in the best case scenario) and for future industrialization of the product it could only be used as a quality confirmation test as opposed to a production control process.

The results of the hardness tests are presented in Fig. 13 below. As expected, the lab test values are slightly better than the production values in the initial stages of production, as laboratory produc-

tion is more precise in its execution than pilot plant production. The patterns of values obtained at 50% RH and 100% RH are almost symmetrical (albeit lower at 100% RH than 50% RH), proving the repeatability of the formulation in a pilot plant production. Finally, there was a constant improvement in the values obtained as production evolved, corresponding to the results obtained by other tests, e.g. the water absorption test.

The rebound hardness (over 7 days per batch) was used only for quality assurance purposes in order to regulate production. In the TUPP case it was clearly used for the evaluation and/or confirmation of the formulation's repeatability. If evaluation of panel hardness is required by the manufacturer during future industrialization of the product then it might be necessary to adopt other tests e.g. use of ultrasonic pulse velocity devices immediately after the panel curing stage.

3.3. Mechanical and durability evaluation of the façade panels developed

Table 5 summarises the test results of the mechanical and physical properties investigated in both laboratory-made samples and those obtained from the pilot production.

It can be seen from the test results presented in Table 5 that panels from each type of production have a similar porosity and density. Bulk density of the alkali activated rendering layer was 1.78 g/cm^3 in panels from the laboratory production compared to 1.81 g/cm^3 from the pilot production. The rendering layer from the laboratory production has a porosity of 25.4%, while the rendering layer from the pilot production has a porosity of 25.5%, which is similar despite slight differences in the mixture composition and panel production method. The rendering layer in panels from the pilot production had an average pore diameter of 0.019 μm which is slightly higher than the equivalent from laboratory production, which was 0.015 μm. Consequently, samples obtained from the pilot production have a slightly higher porosity, higher capillary water absorption and lower water-vapour resistance factor. As shown in Fig. 14, there are no significant changes in the pore distribution of the alkali activated rendering layer in panels produced in the laboratory after 30 cycles of freezing and thawing. The opposite trend can be seen in Fig. 15, where a slightly higher average pore diameter occurred in pilot produced panels after exposure to 30 freeze–thaw cycles. This can be related to micro cracks induced by an increased water volume in solid state.

Table 5
Mechanical and physical properties of the façade panels investigated.

Mechanical parameters	Laboratory panel production	Pilot panel production
Average Pore Diameter (μm)	0.015	0.019
Bulk Density [g/cm^3]	1.78	1.81
Skeletal Density [g/cm^3]	2.38	2.43
Porosity [%]	25.38	25.47
Capillary water absorption test after 24 h [kg/m^2]	1.68	1.81
Watervapour resistance coefficient [/]	59.3	44.5
Water vapour permeability – equivalent air layer thickness [m]	0.6	0.4
Bond strength [MPa]	0.165	0.204
Bond strength after 30 freezethaw cycles [MPa]	0.111	0.164

After 24 h, panels from the pilot production exhibited a capillary water absorption rate of 1.81 kg/m^2, higher than the value of 1.68 kg/m^2 observed in the panels from laboratory production. The values of capillary water absorption for panels from both types of production highly exceeded the limit value of 0.5 kg/m^2 given in ETAG 004 [30]. Therefore, testing of freeze–thaw behaviour is required. Moreover, the water-vapour resistance coefficient was 53.94 for panels from laboratory production and 44.5 for panels from pilot production. The requirements of ETAG 004 [30] give a limit value of 2 m for equivalent air layer thickness when rendering material in combination with cellular plastic insulation. This limit is set in order to reduce the risk of formation of interstitial condensation. It can be seen from the results that the value of equivalent air layer thickness is 0.57 m for laboratory-produced panels and 0.42 m for panels from the pilot production, neither of which exceed the limit given in ETAG 004. It is well known that a high water absorption coefficient and water vapour permeability of rendering material can cause higher penetration of water and water vapour into internal façade layers, which can lead to poor

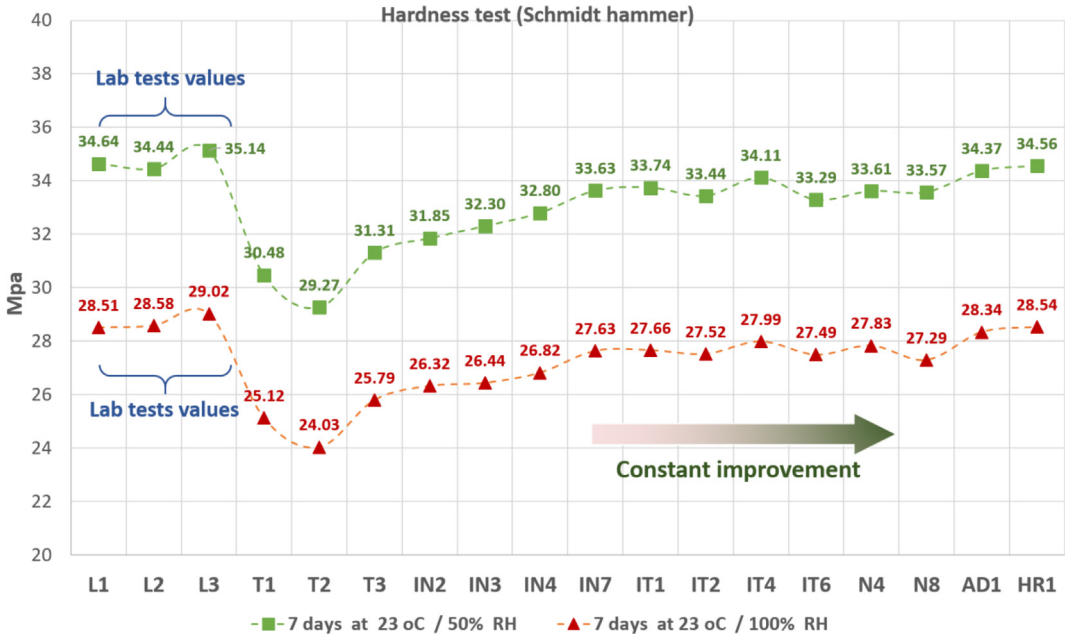

Fig. 13. Schmidt hammer test pattern per batch.

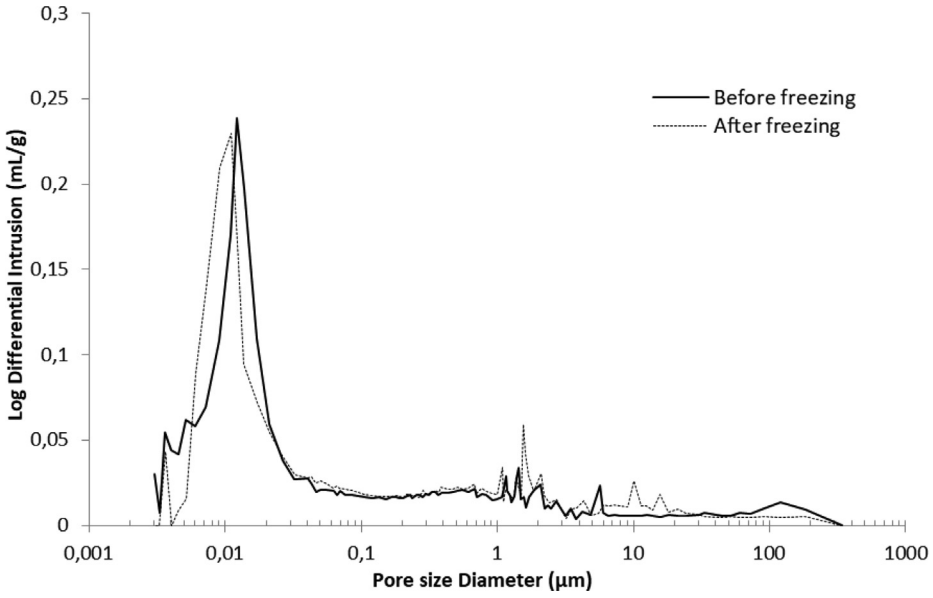

Fig. 14. Pore distribution in the rendering layer of laboratory produced façade samples.

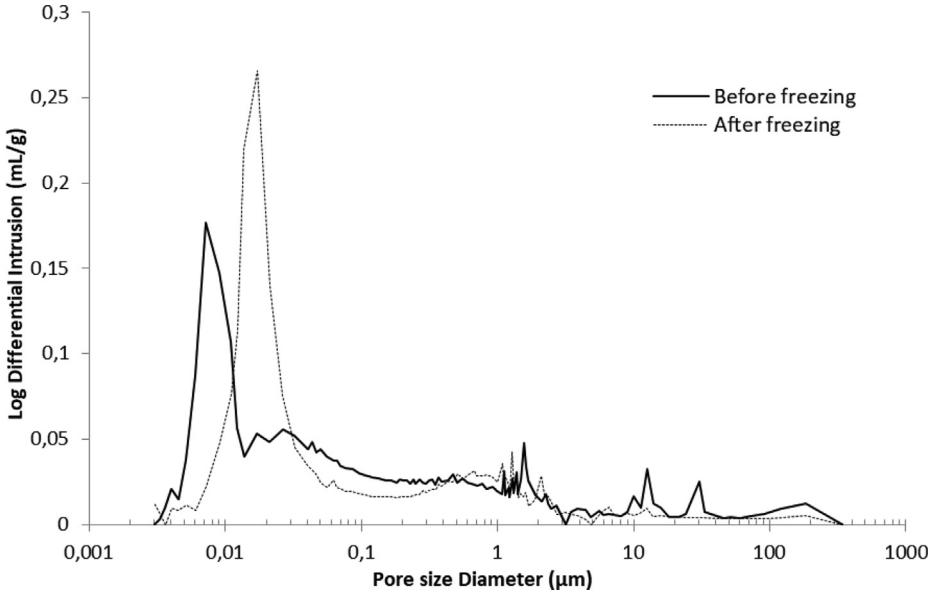

Fig. 15. Pore distribution in the rendering layer of pilot produced façade samples.

freeze–thaw resistance of the material, mould growth, condensation, and a decrease in the thermal resistance. All these parameters reduce the durability of the façade system and of the building itself [40]. In the summer months drying is faster when the water-vapour resistance co-efficient of the facade structure is lower.

The test results of freeze–thaw resistance behaviour, resistance to freezing in the presence of deicing salt, impact resistance, resistance to carbonation, alkali reactivity of aggregates, and sulphate resistance are summarised in Table 6.

After 30 freeze–thaw cycles there were no visible changes on the surface of the panels from either type of production. Freeze-thaw cycles only led to a deterioration of the bond strength between different layers and, in the case of panels from pilot production, failures occurred in different locations. The bond strength of laboratory-produced panels was 0.165 MPa before freezing and 0.111 MPa after 30 freeze–thaw cycles. After 30 freeze–thaw cycles the failure occurred in the EPS insulation layer in 90% of all cases and at the contact between the AAM rendering layer and the EPS insulation layer in the remaining 10% of cases, indicating that the weakest point is the EPS. The measured bond strength of the panels

Table 6
Summary of durability properties of the investigated façade panels.

Durability parameters	Laboratory panel production	Pilot panel production
Freeze-thaw behaviour	No visible changes	No visible changes
Resistance to freezing in the presence of deicing salt	Not resistant	Not resistant
Impact resistance	Category II	Category II
Resistance to carbonation	No visible carbonation	No visible carbonation
Alkali silica reactivity	Resistant	Resistant
Sulphate resistance	Resistant	Resistant

from pilot production decreased from 0.204 MPa before 30 freeze–thaw cycles to 0.164 MPa afterwards. Before the freeze–thaw cycles, failures in the alkali activated rendering layer occurred where the fibre glass mesh is located in 70% of cases and at the contact between the EPS layer and alkali activated rendering layer in the remaining 30% of cases. This may be explained by the high quality synthetic coating on the glass mesh which protects fibres against alkali and prevents adhesion between the AAM and the fiberglass mash. In the case of panels that were exposed to 30 freeze–thaw cycles, adhesive failure took place in the EPS layer in 80% of all cases and in the contact layer between the EPS and alkali activated rendering layer in 20% of cases, what proved to be the weakest point in the case of laboratory produced panels. Nevertheless, the bond strength values did not exceed the threshold given in ETAG 004 [30], i.e. a bond strength of 0.08 MPa between the base coat and the insulation product.

With regards to impact resistance, panels from both types of production showed no damage after the fall of a steel ball with 3 Joules energy, but slightly cracked when a ball with 10 Joules energy was dropped from a 1.02 m height. According to the requirements of the standard ETAG 004 this classifies the panels into Category II, meaning that panels can be used in a zone liable to impact from thrown or kicked objects, but only in public locations where the height of the panels will limit the size of the impact, or at lower levels where access to the building is primarily for those with some incentive to exercise care [30]. In order to increase the impact resistance of the developed façade panels, use of double fibre-glass mesh in the rendering layer is recommended. Furthermore, it must be noted that the use of double fibre-glass mash decreases bond strength in the AAM layer, which was a critical point in the case of pilot produced panels, and increases the water absorption coefficient of the material, consequently reducing the durability of the panels produced [41].

The penetration of carbonates depends on the degree of CO_2 concentration, porosity, pore solution and the type of gel formed during the course of the chemical reaction between the precursor and the activator. A higher CO_2 concentration causes more intense penetration of carbonates into the material, due to a higher partial pressure in the chamber for exposure. Also, during more intense carbonation different products in mineral phase formation are generated [42]. Considering this, a 1% CO_2 concentration was used in this research to accelerate the process of CO_2 penetration in the AAM. Panels from both types of production showed that the AAM mixture developed was resistant to carbonation, as after 56 days of exposure to 1% CO_2 no pH drop was observed on the freshly broken surface.

Conversely, the rendered AAM is not resistant to exposure to deicing salt. After only 3 freeze–thaw cycles in the presence of a 3% NaCl solution, severe deterioration (surface scaling) of the rendered AAM occurred in both panel production types. The same pattern of material damage was identified in the case of cement pastes tested for behaviour upon freezing after being saturated with 3% NaCl solution, attributed to the high pressure exerted on the material matrix due to the growth of salt solution crystals [43]. For this reason, the panels should not be used in areas where a combination of salt and freezing are present. Albitar et. al. [17] researched the durability of alkali activated material in the presence of an NaCl solution and found that the material tested showed good resistance in an environment where freezing is not present. The national standard SIST 1026 states the maximum value for the average amount of surface material scaling is 0.40 mg/mm^2 after 20 cycles in order for a material to be considered resistant to freezing and thawing in the presence of de-icing salt [32].

The results of length change measurements in samples exposed to Na_2SO_4 solution for 55 weeks from Fig. 16 indicate that it is possible that the alkali activation process in the AAM is still active. These phenomena are possible because of the presence of the elements in the Na_2SO_4 solution which are used to activate the precursor in alkaline-activated materials. In laboratory produced panels, this effect was less distinctive since samples were older, and consequently the alkali activated binder was more stable. This statement was further supported by S. A. Bernal, who stated that the presence of Na_2SO_4 increases the maturity of the binder and has no negative effects on alkali activated material [44]. The methodology used for samples exposed to sulphate solution, as given in standard ASTM C227-10, states the maximum permissible value for exposed material expansion to be 0.01% [38].

Fig. 17shows that the samples were resistant to deterioration by alkali attack given that no significant increase in sample length was detected. In addition, shrinking of the alkali activated rendering material was detected in the case of the laboratory produced panels. The methodology used for determination of the aggregate alkali reactivity, as given in standard ASTM C227-10, states the maximum permissible value for exposed material expansion to

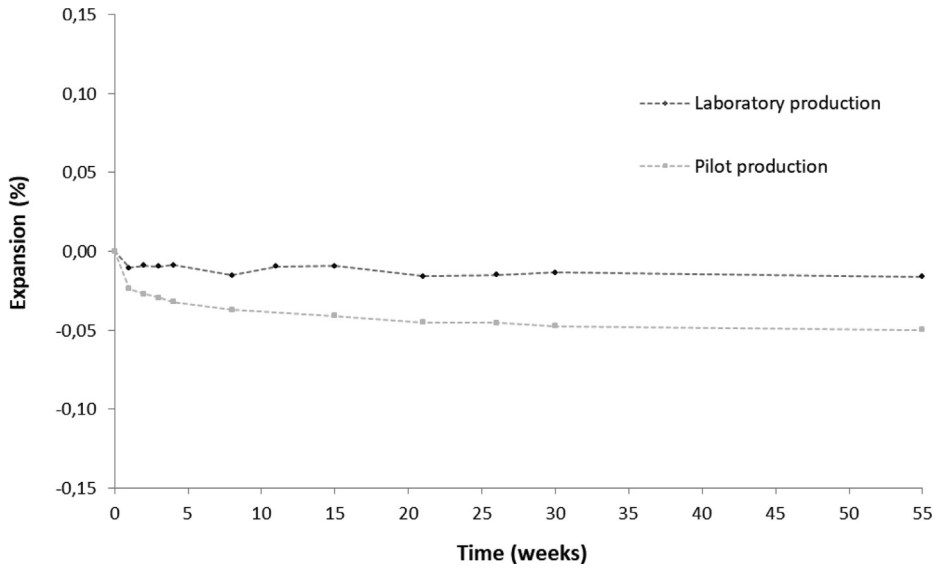

Fig. 16. Length change of samples through 55 weeks of exposure to sulphate solution.

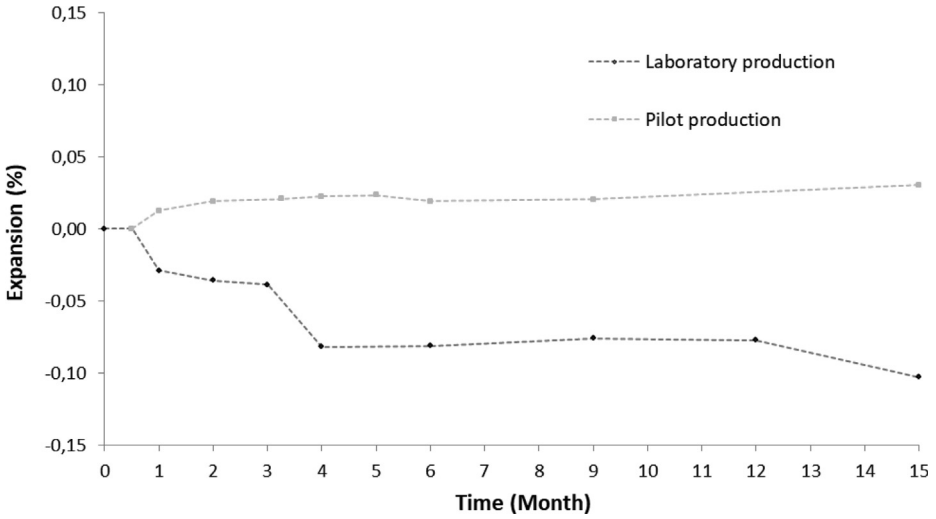

Fig. 17. Length change of samples through 5 months of exposure where potential alkaline reactivity was measured.

be 0.10% [35]. According to literature it is possible for alkali activated materials to develop an alkali silica reaction [45], therefore some additional test might be needed in the case of the AAM from pilot produced panels, where a slight increase in material expansion appeared.

4. Conclusions

As part of the InnoWEE project, ETICS-like panels were produced, first on a laboratory level in dimensions of up to 50 cm × 50 cm, and then upscaled within pilot production in dimensions of 40 cm × 90 cm. Modifications to the mixtures were necessary for the pilot production in order to reduce fluidity and increase setting time while retaining satisfactory performance in terms of strength and drying shrinkage, thus enabling industrial-like semi-automated production of panels. The panels produced in the laboratory and within the pilot production phase have been extensively tested with regard to their mechanical and physical characteristics and durability performance. The following parameters were assessed: capillary water uptake, water vapour permeability, impact resistance, bond strength, freeze–thaw behaviour, freezing in the presence of deicing salt, resistance to carbonation, alkali silica reactivity, and sulphate resistance. Except for the resistance to freezing in the presence of deicing salt, where AAM exhibited severe damage after exposure, all other results were comparable to cement based panels. At 1.02 kg/m^2, water absorption was slightly higher than required in ETAG 004 (where it should be $\leq$ 0.5%), but the testing of freeze–thaw resistance confirmed that there were no cracks or other type of damage after 30 freeze–thaw cycles. By incorporating a mesh into the panels, impact resistance was improved into the "Zone II" group which means that the panels are suitable for zones liable to impact from thrown or kicked objects, but in public locations where the height of the ETICS will limit the size of the impact. Chemical resistance assessed through ASR, carbonation and sulphate exposure tests showed that the rendering layer of the panels developed was resistant to carbonation and that exposure to chemical solutions of sulphate and alkalis did not cause an expansion of the materials beyond the limits set for cement based materials. The experimental results confirmed that panels exhibited a satisfactory performance to be used as façade cladding, with the only exception of areas where freezing in presence of salts may occur. The final confirmation of their suitability will be obtained after the ongoing long-term monitoring of panels installed in demo sites (innowee.eu).

CRediT authorship contribution statement

Ana Frankovič: Investigation, Formal analysis, Writing - original draft. **Vilma Ducman:** Conceptualization, Methodology, Supervision, Writing - review & editing. **Sabina Dolenec:** Methodology, Writing - review & editing. **Matteo Panizza:** Methodology, Investigation, Formal analysis, Writing - review & editing. **Sergio Tamburini:** Conceptualization, Investigation, Supervision, Writing - review & editing. **Marco Natali:** Methodology, Investigation, Writing - review & editing. **Maria Pappa:** Investigation, Formal analysis, Writing - review & editing. **Constantinos Tsoutis:** Methodology, Supervision, Writing - review & editing. **Adriana Bernardi:** Funding acquisition, Supervision, Writing - review & editing.

Declaration of Competing Interest

The authors declare that they have no known competing financial interests or personal relationships that could have appeared to influence the work reported in this paper.

Acknowledgements

This project has received funding from the European Union's Horizon 2020 research and innovation programme under Grant Agreement No. 723916.

References

[1] Eurostat, Generation of waste by waste category, hazardousness and NACE Rev. 2 activity, (2018).
[2] R. Smith, Directive 2008/98/EC of the European Parliament and of the Council of 19 November 2008, in: Core EU Legislation, Macmillan Education UK, London, 2015: pp. 426–429. https://doi.org/10.1007/978-1-137-54482-7_45.
[3] F.P. Torgal (Ed.), Handbook of recycled concrete and demolition waste, Woodhead Pub, Cambridge; Philadelphia, 2013.
[4] J.L. Provis, J.S.J. van Deventer, Geopolymers and Other Alkali-Activated Materials, in: Lea's Chemistry of Cement and Concrete, Elsevier, 2019: pp. 779–805. https://doi.org/10.1016/B978-0-08-100773-0.00016-2.
[5] S. Kramar, A. Šajna, V. Ducman, Assessment of alkali activated mortars based on different precursors with regard to their suitability for concrete repair, Constr. Build. Mater. 124 (2016) 937–944, https://doi.org/10.1016/j.conbuildmat.2016.08.018.
[6] L. Reig, M.M. Tashima, M.V. Borrachero, J. Monzó, C.R. Cheeseman, J. Payá, Properties and microstructure of alkali-activated red clay brick waste, Constr.

Build. Mater. 43 (2013) 98–106, https://doi.org/10.1016/j.conbuildmat.2013.01.031.
[7] M. Panizza, M. Natali, E. Garbin, S. Tamburini, M. Secco, Assessment of geopolymers with Construction and Demolition Waste (CDW) aggregates as a building material, Constr. Build. Mater. 181 (2018) 119–133, https://doi.org/10.1016/j.conbuildmat.2018.06.018.
[8] L. Reig, M.A. Sanz, M.V. Borrachero, J. Monzó, L. Soriano, J. Payá, Compressive strength and microstructure of alkali-activated mortars with high ceramic waste content, Ceram. Int. 43 (2017) 13622–13634, https://doi.org/10.1016/j.ceramint.2017.07.072.
[9] A. Mohammadinia, A. Arulrajah, J. Sanjayan, M.M. Disfani, M.W. Bo, S. Darmawan, Strength Development and Microfabric Structure of Construction and Demolition Aggregates Stabilized with Fly Ash-Based Geopolymers, J. Mater. Civ. Eng. 28 (2016) 04016141, https://doi.org/10.1061/(ASCE)MT.1943-5533.0001652.
[10] K. Komnitsas, D. Zaharaki, A. Vlachou, G. Bartzas, M. Galetakis, Effect of synthesis parameters on the quality of construction and demolition wastes (CDW) geopolymers, Adv. Powder Technol. 26 (2015) 368–376, https://doi.org/10.1016/j.apt.2014.11.012.
[11] S. Ahmari, X. Ren, V. Toufigh, L. Zhang, Production of geopolymeric binder from blended waste concrete powder and fly ash, Constr. Build. Mater. 35 (2012) 718–729, https://doi.org/10.1016/j.conbuildmat.2012.04.044.
[12] A. Vásquez, V. Cárdenas, R.A. Robayo, R.M. de Gutiérrez, Geopolymer based on concrete demolition waste, Adv. Powder Technol. 27 (2016) 1173–1179, https://doi.org/10.1016/j.apt.2016.03.029.
[13] A. Allahverdi, E.N. Kani, Construction Wastes as Raw Materials for Geopolymer Binders, International Journal of Civil Engineering. 7 (2009) 8.
[14] R. Vinai, M. Soutsos, Production of sodium silicate powder from waste glass cullet for alkali activation of alternative binders, Cem. Concr. Res. 116 (2019) 45–56, https://doi.org/10.1016/j.cemconres.2018.11.008.
[15] N. Toniolo, A. Rincón, J.A. Roether, P. Ercole, E. Bernardo, A.R. Boccaccini, Extensive reuse of soda-lime waste glass in fly ash-based geopolymers, Constr. Build. Mater. 188 (2018) 1077–1084, https://doi.org/10.1016/j.conbuildmat.2018.08.096.
[16] M. Torres-Carrasco, F. Puertas, Waste glass in the geopolymer preparation. Mechanical and microstructural characterisation, J. Cleaner Prod. 90 (2015) 397–408, https://doi.org/10.1016/j.jclepro.2014.11.074.
[17] M. Albitar, M.S. Mohamed Ali, P. Visintin, M. Drechsler, Durability evaluation of geopolymer and conventional concretes, Constr. Build. Mater. 136 (2017) 374–385, https://doi.org/10.1016/j.conbuildmat.2017.01.056.
[18] N. Singh, S. Vyas, R.P. Pathak, P. Sharma, N.V. Mahure, S.L. Gupta, Effect of Aggressive Chemical Environment on Durability of Green Geopolymer, Concrete 3 (2013) 8.
[19] I. Ismail, S.A. Bernal, J.L. Provis, S. Hamdan, J.S.J. van Deventer, Microstructural changes in alkali activated fly ash/slag geopolymers with sulfate exposure, Mater Struct. 46 (2013) 361–373, https://doi.org/10.1617/s11527-012-9906-2.
[20] A. Nazari, A. Bagheri, J.G. Sanjayan, M. Dao, C. Mallawa, P. Zannis, S. Zumbo, Thermal shock reactions of Ordinary Portland cement and geopolymer concrete: Microstructural and mechanical investigation, Constr. Build. Mater. 196 (2019) 492–498, https://doi.org/10.1016/j.conbuildmat.2018.11.098.
[21] M. Nedeljković, B. Šavija, Y. Zuo, M. Luković, G. Ye, Effect of natural carbonation on the pore structure and elastic modulus of the alkali-activated fly ash and slag pastes, Constr. Build. Mater. 161 (2018) 687–704, https://doi.org/10.1016/j.conbuildmat.2017.12.005.
[22] K. Pasupathy, M. Berndt, A. Castel, J. Sanjayan, R. Pathmanathan, Carbonation of a blended slag-fly ash geopolymer concrete in field conditions after 8years, Constr. Build. Mater. 125 (2016) 661–669, https://doi.org/10.1016/j.conbuildmat.2016.08.078.
[23] P. Sun, H.-C. Wu, Chemical and freeze–thaw resistance of fly ash-based inorganic mortars, Fuel 111 (2013) 740–745, https://doi.org/10.1016/j.fuel.2013.04.070.
[24] J. Provis, Alkali activated materials: state-of-the-art report, RILEM TC 224-AAM, Springer, New York, 2013.
[25] Official Journal of the European Union. (2010) (n.d.) 23.
[26] E. Franzoni, B. Pigino, G. Graziani, C. Lucchese, A. Fregni, A new prefabricated external thermal insulation composite board with ceramic finishing for buildings retrofitting, Mater Struct. 49 (2016) 1527–1542, https://doi.org/10.1617/s11527-015-0593-7.
[27] EU Commission Decision of 18 December 2014 n. 2014/955/EU, Official Journal of the European Union n. L 370/44, (2014).
[28] EN 12457-2:2004, Characterisation of waste - Leaching - Compliance test for leaching of granular waste materials and sludges - Part 2: One stage batch test at a liquid to solid ratio of 10 l/kg for materials with particle size below 4 mm (without or with size reduction), n.d.
[29] D.e. Feo, A. Joseph, W. Barnard, JURAN,, Institute's Six Sigma Breakthrough and Beyond - Quality Performance Breakthrough Methods, Tata McGraw-Hill Publishing Company Limited, 2005.
[30] ETAG 004, Guideline for European technical approval of external thermal insulation composite system (ETICS) with rendering, n.d.
[31] EN ISO 7783:2012, Paints and varnishes - Determination of water - vapour transmission properties - Cup method (ISO 7783:2011), n.d.
[32] SIST 1026:2016, Concrete – Specification, performance, production and conformity – Rules for the implementation of SIST EN 206, n.d.
[33] ISO 7892:1988, Vertical building elements - Impact resistance tests - Impact bodies and general test procedures, n.d.
[34] EN 13295:2004, Products and systems for the protection and repair of concrete structures – test methods – Determination of resistance to carbonation, n.d.
[35] ASTM C227-10, Standard Test Method for Potential Alkali Reactivity of Cement-Aggregate Combinations (Mortar-Bar Method), n.d.
[36] ASTM C1012/C1012M – 09, Standard Test Method for Length Change of Hydraulic-Cement Mortars Exposed to a Sulfate Solution, n.d.
[37] M. Lizcano, A. Gonzalez, S. Basu, K. Lozano, M. Radovic, Effects of Water Content and Chemical Composition on Structural Properties of Alkaline Activated Metakaolin-Based Geopolymers, J. Am. Ceram. Soc. 95 (2012) 2169–2177, https://doi.org/10.1111/j.1551-2916.2012.05184.x.
[38] J.L. Provis, Alkali-activated materials, Cem. Concr. Res. 114 (2018) 40–48, https://doi.org/10.1016/j.cemconres.2017.02.009.
[39] M. Mastali, P. Kinnunen, A. Dalvand, R. Mohammadi Firouz, M. Illikainen, Drying shrinkage in alkali-activated binders – A critical review, Constr. Build. Mater. 190 (2018) 533–550, https://doi.org/10.1016/j.conbuildmat.2018.09.125.
[40] J. Zhao, F. Meissener, Experimental investigation of moisture properties of historic building material with hydrophobization treatment, Energy Procedia 132 (2017) 261–266, https://doi.org/10.1016/j.egypro.2017.09.716.
[41] R. Norvaišienė, G. Griciutė, R. Bliūdžius, J. Ramanauskas, The Changes of Moisture Absorption Properties during the Service Life of External Thermal Insulation Composite System, Ms. 19 (2013) 103–107, https://doi.org/10.5755/j01.ms.19.1.3834.
[42] S.A. Bernal, J.L. Provis, B. Walkley, R. San Nicolas, J.D. Gehman, D.G. Brice, A.R. Kilcullen, P. Duxson, J.S.J. van Deventer, Gel nanostructure in alkali-activated binders based on slag and fly ash, and effects of accelerated carbonation, Cem. Concr. Res. 53 (2013) 127–144, https://doi.org/10.1016/j.cemconres.2013.06.007.
[43] Q. Zeng, T. Fen-Chong, K. Li, Freezing behavior of cement pastes saturated with NaCl solution, Constr. Build. Mater. 59 (2014) 99–110, https://doi.org/10.1016/j.conbuildmat.2014.02.042.
[44] S.A. Bernal, J.L. Provis, Durability of Alkali-Activated Materials: Progress and Perspectives, J. Am. Ceram. Soc. 97 (2014) 997–1008, https://doi.org/10.1111/jace.12831.
[45] Z. Shi, C. Shi, R. Zhao, S. Wan, Comparison of alkali–silica reactions in alkali-activated slag and Portland cement mortars, Mater Struct. 48 (2015) 743–751, https://doi.org/10.1617/s11527-015-0535-4.